Published in IET Microwaves, Antennas & Propagation
Received on 7th August 2007
Revised on 15th February 2008
doi: 10.1049/iet-map:20070180

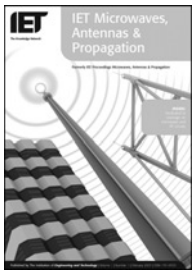

ISSN 1751-8725

Study and realisation of dual-composite right/left-handed coplanar waveguide metamaterial in MMIC technology

W. Tong[1] *Z. Hu*[1] *H. Zhang*[2] *C. Caloz*[3] *A. Rennings*[4]

[1]*School of Electrical and Electronic Engineering, The University of Manchester, PO box 88, Manchester M60 1QD, UK*
[2]*Department of MMICs and Compound Semiconductor Devices, Institute of Microelectronics, Chinese Academy of Science, People's Republic of China*
[3]*Ecole Polytechnique de Montreal, 2500, Ch. De Polytechnique, Montreal, Quebec H3T 1J4, Canada*
[4]*IMST, Carl-Friedrich-Gauβ-Str. 2, Kamp-Lintfort D-47475, Germany*
E-mail: tw19820507@yahoo.com.cn

Abstract: A novel realisable dual composite right/left-handed (D-CRLH) coplanar waveguide (CPW) transmission line (TL) in GaAs MMIC technology demonstrated by theoretical analysis and experimental results is presented. A D-CRLH TL is the dual of the conventional CRLH TL in the sense that it consists of series LC parallel tanks and shunt LC series tanks. However, an ideal D-CRLH TL cannot be realised because of unavoidable parasitic effects. The measured results indicated that a real D-CRLH TL exhibits a fundamentally different frequency response at higher frequency band in that a real D-CRLH TL cannot provide unlimited left handed (LH) bandwidth. Instead, it has triple bands; right-handed (RH) passband at lower frequencies (DC-2.9 GHz), LH passband at intermediate frequencies (5.1–14.3 GHz) and RH passband at higher frequencies (above 14.3 GHz). The reported fully integrated D-CRLH CPW TL metamaterial has a very compact size of 2.2 mm^2 which leads to a small loss 1.5 dB within 3 dB LH passband.

1 Introduction

Metamaterial exhibiting simultaneously negative permeability and negative permittivity, called left-handed (LH) metamaterial, was theoretically predicted by Veselago [1] in the late 1960s and has recently attracted much attention. In particular, LH transmission line (TL) metamaterials have made this new media practical for RF/microwave circuit implementations [2–4]. These LH TL metamaterials typically exhibit a LH passband at lower frequencies and right-handed (RH) passband at higher frequencies and have already led to many applications [5–10].

Dual to composite right/left-handed (CRLH) TL, a novel TL metamaterial with series LC parallel tank and shunt LC series tank, termed dual CRLH (D-CRLH) was proposed in [11] and further investigated in [12]. However, a D-CRLH TL is ideal and cannot be realised in practice since RH parasitic effects are unavoidable. Instead of providing unlimited LH passband at higher frequencies, a practically realisable D-CRLH TL exhibits triple operating passbands [13], where a printed circuit board (PCB) microstrip technology was used for implementing the D-CRLH TL. In this paper, we have advanced the PCB to GaAs monolithic millimetre-wave integrated circuit (MMIC) technology in realising the D-CRLH TLs. The fully integrated D-CRLH TL based on MMIC technology offers not only compact size, but also significant reduction in RH parasitic effects. The fabricated CPW MMIC D-CRLH TL occupies only 1.35% area of that reported in [13]. Thanks to the miniaturised size and CPW structure, the RH parasitic effects of the TL are rather small, leading to a 3.5 times broader LH operating bandwidth.

2 Theoretical analysis of D-CRLH TL unit cell

The equivalent circuit model for the unit cell of a D-CRLH TL is shown in Fig. 1. It is constructed by a series LC parallel tank (C_L, L_R) and a shunt LC series tank (C_R, L_L). Taking into account the RH effects of the D-CRLH TL, the

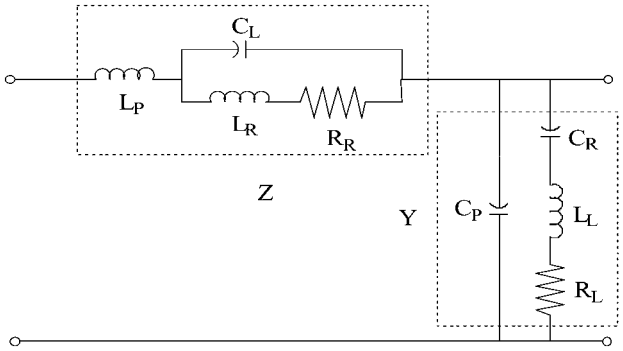

Figure 1 *Equivalent circuit model for a realisable D-CRLH TL metamaterial*

The subscripts R and L stand for right-handed (RH) and left-handed (LH), respectively
C_P and L_P are parasitic capacitance and inductance
R_R and R_L represent the losses of the spiral inductors

parasitic series inductance L_P and shunt capacitance C_P have been included in the equivalent circuit model. Although the values of these parasitic inductor and capacitor may be small, especially in MMIC technology, the existence of such parasitic components has fundamentally changed the D-CRLH TL property in that it can no longer have an unlimited LH passband at higher frequencies. The resistors R_R and R_L account for losses of the spiral inductors of L_R and L_L, respectively. The losses of L_P have been ignored since the unavoidable RH TL is very short.

For an ideal D-CRLH TL, where resistors R_R, R_L, parasitic series inductor L_P and shunt C_P are all zero, the series parallel LC tank is inductive below f_{se} ($f_{se} = 1/2\pi\sqrt{L_R C_L}$) and capacitive above f_{se}, whereas the shunt series LC tank is capacitive below f_{sh} ($f_{sh} = 1/2\pi\sqrt{C_R L_L}$) and inductive above f_{sh}, as illustrated in Fig. 2. At lower frequencies, for $f < \min(f_{se}, f_{sh})$, the dominant components are L_R and C_R, which leads to the response of a conventional RH TL. In contrast, at higher frequencies, $f > \max(f_{se}, f_{sh})$, the dominant components are C_L and L_L, so that the TL behaves as LH TL and has an unlimited LH bandwidth.

For a realisable D-CRLH TL, due to the existence of RH parasitic effects, the dominant components become L_P and C_P at higher frequency, so that the TL no longer has an unlimited LH bandwidth, but behaves as RH TL again. Thus, a realisable D-CRLH exhibits a low-frequency RH band, an intermediate-frequency LH band and a high-frequency RH band.

For a lossy D-CRLH TL unit cell, the series impedance Z and shunt admittance Y, as shown in Fig. 1 can be derived as

$$Z = j\omega L_P + \frac{1}{j\omega C_L} // \left(j\omega L_R + R_R\right) = j\omega L_P \times \frac{\omega^2 - \omega_{0,\text{lossless}}^{se^2} - \left((j\omega R_R/L_R) + (R_R/j\omega C_L L_P L_R)\right)}{\omega^2 - \omega_{\infty,\text{lossless}}^{se^2} - (j\omega R_R/L_R)} \quad (1a)$$

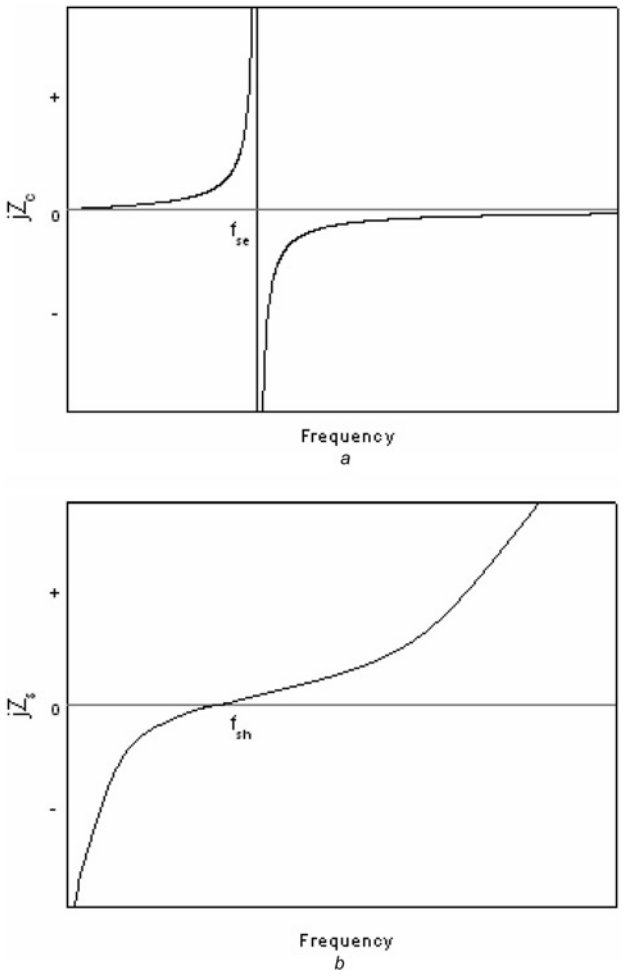

Figure 2 *Response of the tanks*

a Parallel LC tank
b Series LC tank

$$Y = j\omega C_P + j\omega C_R // \frac{1}{j\omega L_L} // \frac{1}{R_L} = j\omega C_P \frac{\omega^2 - \omega_{0,\text{lossless}}^{sh^2} - j\omega(R_L/L_L)}{\omega^2 - \omega_{\infty,\text{lossless}}^{sh^2} - j\omega(R_L/L_L)} \quad (1b)$$

where

$$\omega_{\infty,\text{lossless}}^{se} = \frac{1}{\sqrt{L_R C_L}} \quad (2a)$$

$$\omega_{0,\text{lossless}}^{se} = \sqrt{\frac{L_R + L_P}{L_R L_P C_L}} \quad (2b)$$

$$\omega_{\infty,\text{lossless}}^{sh} = \frac{1}{\sqrt{L_L C_R}} \quad (2c)$$

$$\omega_{0,\text{lossless}}^{sh} = \sqrt{\frac{C_R + C_P}{L_L C_P C_R}} \quad (2d)$$

The complex propagation constant γ, with its attenuation factor α and phase constant β, and the complex characteristic impedance Z_0 of the D-CRLH TL unit cell

doi: 10.1049/iet-map:20070180

can be obtained by

$$\gamma(\omega) = \alpha(\omega) + j\beta(\omega) = \sqrt{ZY} \tag{3a}$$

$$Z_0(\omega) = \sqrt{\frac{Z}{Y}} \tag{3b}$$

Fig. 3 shows typical dispersion diagrams for a lossy D-CRLH TL unit cell, which are calculated from (1) and (3), with parameter values of $L_P = 0.15$ nH, $C_P = 0.075$ pF, $C_R = 1$ pF, $C_L = 0.9$ pF, $L_L = 1.8$ nH, $L_R = 2.3$ nH, $R_R = 3.5\ \Omega$ and $R_L = 3\ \Omega$. It can be seen that a clear bandstop filtering effect is demonstrated. The D-CRLH TL exhibits interesting tri-band performance: RH passband at lower frequencies, LH passband at intermediate frequencies and RH passband at higher frequencies.

3 Equivalent circuit model simulation and analysis of D-CRLH TL

The equivalent circuit model in Fig. 1 is used to analyse the D-CRLH TL transmission and dispersion characteristics of the D-CRLH TL. It is noticed that the equivalent circuit model has taken into account the losses of R_R and R_L, caused mainly by the thin inductor lines. The transmission characteristics of a lossy D-CRLH TL with five unit cells are shown in Fig. 4. It can be seen that the S_{21} becomes smoother but less sharp at bandstop filtering eigen-frequencies as the losses increase. Moreover, as shown in Fig. 5, as the losses increase, the cutoff frequency $\omega^{se}_{\infty,loss}$ moves to lower frequencies and $\omega^{sh}_{\infty,loss}$ moves to higher frequencies, resulting in further apart from the first RH passband at lower frequency and LH passband at intermediate frequency. It is noticed that in the case of low loss, $\omega^{se}_{\infty,loss}$ and $\omega^{sh}_{\infty,loss}$ are close to those of the lossless case $\omega^{se}_{\infty,lossless}$ and $\omega^{sh}_{\infty,lossless}$, respectively, which indicates that the analytical expresses for a lossless D-CRLH TL can be used for low loss case.

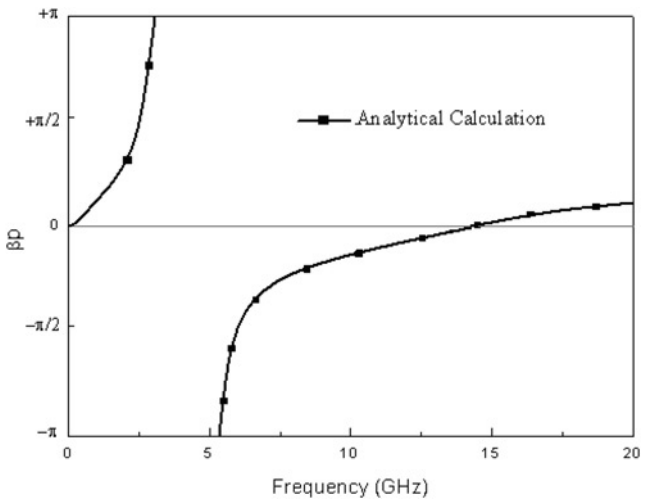

Figure 3 *Dispersion diagram of a lossy D-CRLH TL, which is calculated from (1) and (3) with parameters of $L_P = 0.15$ nH, $C_P = 0.075$ pF, $C_R = 1$ pF, $C_L = 0.9$ pF, $L_L = 1.8$ nH, $L_R = 2.3$ nH, $R_R = 3.5\ \Omega$ and $R_L = 3\Omega$*

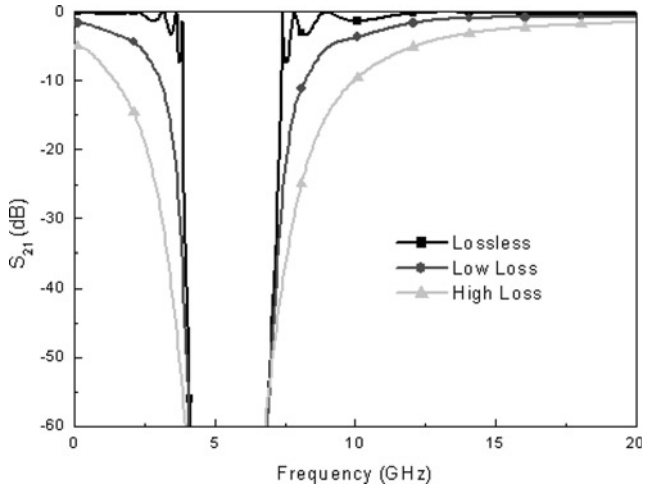

Figure 4 *Effects of loss in the transmission characteristic of the D-CRLH TL with five unit cells*

The parameters of the unit cell are $L_P = 0.2$ nH, $C_P = 0.12$ pF, $C_R = 1$ pF, $C_L = 0.6$ pF, $L_L = 0.9$ nH, $L_R = 1.5$ nH
R_R and R_L are of 4 Ω for low loss case and 15 Ω for high loss case, respectively

Thus, for a low loss D-CRLH TL, (1) can be reduced to

$$Z = j\omega L_P \frac{\omega^2 - \omega^{se2}_{0,lossless}}{\omega^2 - \omega^{se2}_{\infty,lossless}} \tag{4a}$$

$$Y = j\omega C_P \frac{\omega^2 - \omega^{sh2}_{0,lossless}}{\omega^2 - \omega^{sh2}_{\infty,lossless}} \tag{4b}$$

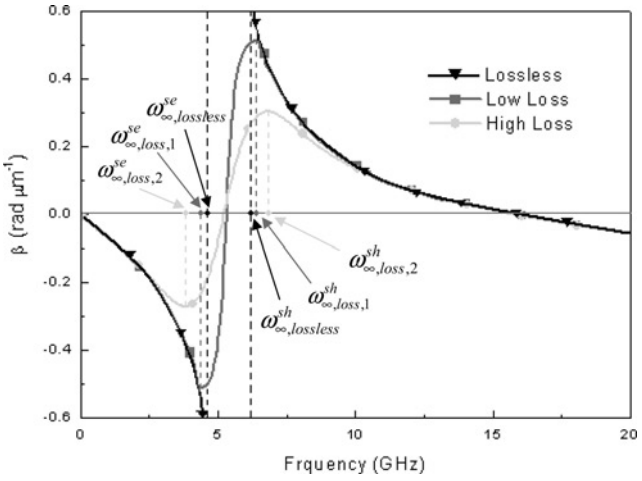

Figure 5 *Effects of loss in the dispersion of the D-CRLH TL with five unit cells*

The parameters of the unit cell are $L_P = 0.2$ nH, $C_P = 0.12$ pF, $C_R = 1$ pF, $C_L = 0.6$ pF, $L_L = 0.9$ nH, $L_R = 1.5$ nH
R_R and R_L are of 4 Ω for low loss case and 15 Ω for high loss case, respectively. The index '1' and '2' indicate cases of low loss and high loss, respectively

which become the same as that derived in [13]. The complex propagation constant γ, with its attenuation factor α and phase constant β, and the complex characteristic impedance Z_0 of the D-CRLH TL can be obtained from (3) and (4) as

$$\gamma(\omega) = \mathrm{j}s(\omega)\frac{\omega}{\omega_P}\sqrt{\frac{(\omega^2-\omega^{se2}_{0,lossles})(\omega^2-\omega^{sh2}_{0,lossless})}{(\omega^2-\omega^{se2}_{\infty,lossless})(\omega^2-\omega^{sh2}_{\infty,lossless})}} \quad (5a)$$

$$Z_0(\omega) = \sqrt{\frac{L_P}{C_P}}\sqrt{\frac{(\omega^2-\omega^{se2}_{0,lossless})(\omega^2-\omega^{sh2}_{\infty,lossless})}{(\omega^2-\omega^{se2}_{\infty,lossless})(\omega^2-\omega^{sh2}_{0,lossless})}} \quad (5b)$$

Where

$$\omega_P = \frac{1}{\sqrt{L_P C_P}} \quad (5c)$$

The $s(\omega)$ is a sign function of (± 1), which indicates positive for RH region and negative for LH region. In the balanced case, where $\omega^{se}_{0,lossless} = \omega^{sh}_{0,lossless} = \omega_0$ and $\omega^{se}_{\infty,lossless} = \omega^{sh}_{\infty,lossless} = \omega_\infty$, one has

$$\beta(\omega) = \frac{\omega}{\omega_P}\frac{\omega^2-\omega_0^2}{\omega^2-\omega_\infty^2} \quad (6a)$$

$$Z_0 = \sqrt{\frac{L_L}{C_L}} = \sqrt{\frac{L_R}{C_R}} \quad (6b)$$

Thus, in this case, characteristic eigen-frequencies of such D-CRLH TL consist of one zero at the origin $[\beta(\omega = 0) = 0]$, two poles and two zeros deciding the cutoff frequencies of the gap, $[\beta(\omega = \omega^{se}_{\infty,lossless}, \omega^{sh}_{\infty,lossless}) = \infty]$ and $[\beta(\omega = \omega^{se}_{0,lossless}, \omega^{sh}_{0,lossless}) = 0]$, respectively.

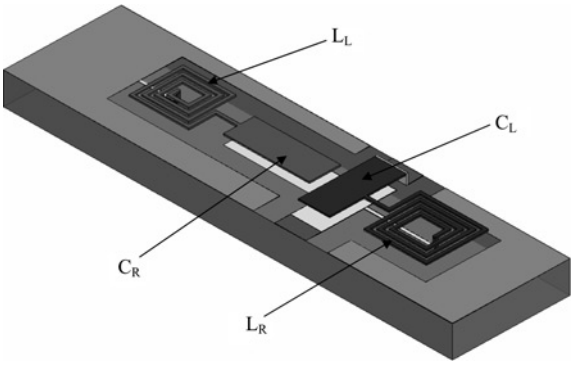

Figure 6 *Layout of the unit cell of the D-CRLH TL in GaAs MMIC technology*

The polyimide layer sandwiched between two metal layers has a dielectric constant of 3.8
All the strips and gaps for the spiral inductors are 15 μm

4 Experimental results

The layout of the unit cell of the D-CRLH TL in MMIC technology is shown in Fig. 6. The capacitance and inductance are typically implemented under the form of parallel metal plane capacitors and spiral inductors.

The fully integrated D-CRLH TL metamaterial was constructed by cascading five D-CRLH unit cells on a GaAs substrate. The thickness of the GaAs substrate is of 625 μm. Ti/Au metallisation was formed by first evaporating Ti thin film onto the substrate then Au metal layer is deposited onto the Ti layer. The polyimide layer is spun on the Ti/Au metal layer and cured under the vacuum oven at 200°C for 2 h. The thickness of the polyimide layers is about 1 μm and the relative dielectric constant is about 3.8. The vias were formed using oxygen plasma reactive ion etching. This is then followed by evaporating the next Ti/Au metal layer. The physical dimensions of the spiral inductors are shown in Table 1. The CPW line dimensions were selected to give a nominal 50 Ω characteristic impedance and to accommodate 200 μm pitch ground-signal-ground (GSG) CPW probes, with the line spacing of 70 μm and a signal line width of 100 μm.

The fabricated fully integrated D-CRLH TL with five unit cells is shown in Fig. 7. Thanks to MMIC technology, the fabricated CPW D-CRLH TL has a size of 2.2 mm^2, which is only 1.35% of that realised using a PCB microstrip technology [13]. The measurements were

Table 1 Physic dimensions of the fabricated 1.8 and 2.3 nH spiral inductors (t_1 is the thickness of bottom layer of metal and t_2 is for top layer)

Inductor	Turns *n*	Width *w*, μm	Diameter *d*, μm	Spacing *s*, μm	Thickness, μm	
					t_1	t_2
1.8 nH	2.5	15	230	15	1	3
2.3 nH	2.5	15	280	15	1	3

doi: 10.1049/iet-map:20070180

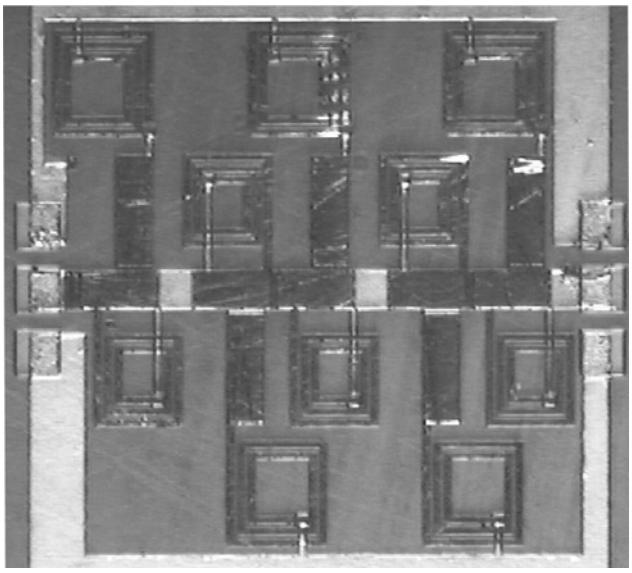

Figure 7 *Fabricated D-CRLH TL with five unit cells*

carried out using HP 85107A vector network analyser and Cascade wafer probe station with 200 μm GSG coplanar probes calibrated using line reflect match (LRM) to the probe tips. The measured scattering parameters are shown in Fig. 8. It can be seen that a very good agreement between the measured and simulation results, from both equivalent circuit model and full-wave simulation, has been achieved. It can also be seen that the MMIC CPW D-CRLH TL has a small insertion loss <1.5 dB within the 3 dB passband, and a very deep stopband, better than −30 dB rejection.

Fig. 9 illustrates the dispersion characteristics of the D-CRLH TL, obtained by unwrapping the phase of S_{21} as $\beta = -\Phi\{S_{21}\}/p$, where p is the line length [5]. The negative sign of the slope for a negative wave number from 5.1 to 14.3 GHz demonstrates the existence of a negative phase velocity in this frequency range. It can be seen that the structure exhibits a low-frequency RH band from 0 to

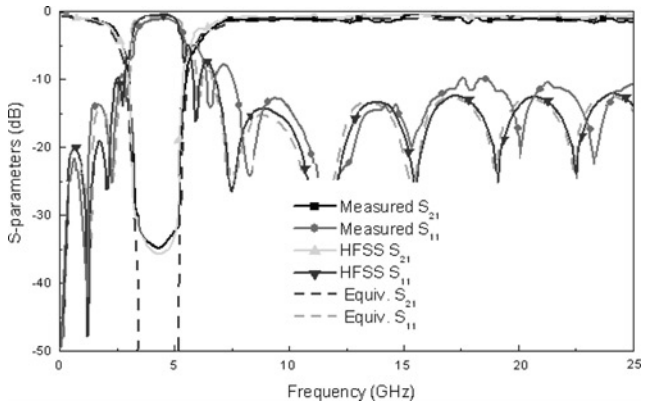

Figure 8 *Transmission and reflection coefficients of the fabricated D-CRLH with five unit-cells*

The parameters are $L_P = 0.15$ nH, $C_P = 0.075$ pF, $C_R = 1$ pF, $C_L = 0.9$ pF, $L_L = 1.8$ nH, $L_R = 2.3$ nH, $R_R = 1.62\ \Omega$ and $R_L = 2.16\ \Omega$

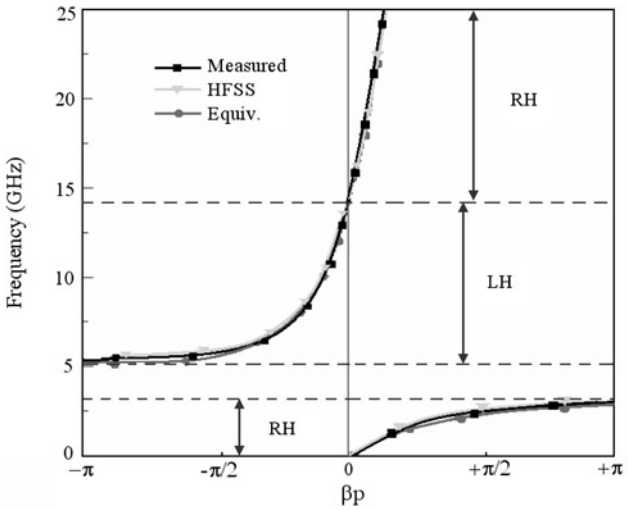

Figure 9 *Dispersion diagram of the fabricated D-CRLH TL with five unit-cells, where p is the total length of the line*

2.9 GHz, an intermediate-frequency LH band from 5.1 to 14.3 GHz and a high-frequency RH band above 14.3 GHz. Thus, the intermediate-frequency LH bandwidth is 3.5 times broader than that of a microstrip PCB structure [13], because of the small RH parasitic effects in MMIC technology.

5 Conclusion

A novel D-CRLH TL in GaAs MMIC technology is presented. The triple bands of such TL, a low-frequency RH band, an intermediate-frequency LH band and a high-frequency RH band, are demonstrated theoretically and experimentally. Thanks to the applications of MMIC technology, such TL has a rather compact size of 2.2 mm^2, which is only 1.35% to that reported in [13]. Furthermore, due to the compact size and CPW structure, RH effects have been significantly reduced, leading to a 3.5 times broader LH bandwidth than that of a PCB microstrip. However, the RH parasitic C_P and L_P cannot be ignored even though they can be reduced to very small. Thus, a practical D-CRLH TL will be dominated again by RH effect at the higher frequencies.

6 Acknowledgment

This project is supported by United Kingdom's Engineering and Physical Science Research Council (UK EPSRC) under Grant EP/C015339/1. W. Tong also wishes to acknowledge the financial support of UK EMRS DTC, the University of Manchester and ORS for his PhD study.

7 References

[1] VESELAGO V.G.: 'The electrodynamics of substances with simultaneously negative value of ε and μ' (in Russian), *Sov. Phys. Uspekhi*, 1968, **10**, (4), pp. 509–514

[2] CALOZ C., ITOH T.: 'Application of the transmission line theory of left-handed (LH) materials to the realization of a microstrip LH line'. IEEE AP-S/URSI Int. Symp. Dig, San Antonio, TX, June 2002, pp. 412–415

[3] IYER A.K., ELEFTHERIADES G.V.: 'Negative refractive index media supporting 2-D waves'. IEEE MTT-S Int. Microwave Symp. Dig, June 2002, pp. 1067–1070

[4] OLINER A.A.: 'A periodic-structure negative-refractive-index medium without resonant elements'. IEEE AP-S/URSI Int. Symp. Dig., San Antonio, TX, June 2002, pp. 41–44

[5] CALOZ C., ITOH T.: 'Electromagnetic metamaterials: transmission line theory and microwave applications' (Wiley and IEEE Press, New York, 2005)

[6] ANTONIADES M.A., ELEFTHERIADES G.V.: 'A broadband wilkinson balun using microstrip metamaterial lines', *IEEE Antennas Wirel. Propag. Lett.*, 2005, **4**, pp. 209–212

[7] TONG W., HU Z.: 'Left-handed L band bandstop filter with significantly reduced-size', *IEE Proc. Antennas Propag.*, 2007, **1**, pp. 45–49

[8] MAO S.G., WU M.S., CHUEH Y.Z., CHEN C.H.: 'Modeling of symmetric composite right/left-handed coplanar waveguides with applications to compact bandpass filters', *IEEE Trans. Microw. Theory. Tech.*, 2005, **53**, (11), pp. 3460–3465

[9] NGUYEN H.V., CALOZ C.: 'Generalized coupled-mode approach of metamaterial coupled-line couplers: coupling theory, phenomenological explanation, and experimental demonstration', *IEEE Trans. Microw. Theory. Tech.*, 2005, **55**, pp. 1029–1039

[10] SAENZ E., CANTORA A., EDERRA I., GONZALO R., JACKSON D.R., WILTON D.R.: 'A metamaterial T-junction power divider', *Microw. Wirel. Compon. Lett.*, 2007, **17**, pp. 172–174

[11] CALOZ C.: 'Dual composite right/left-handed (D-CRLH) transmission line metamaterial', *Microw. Wirel. Compon. Lett.*, 2006, **16**, pp. 585–587

[12] CALOZ C., NGUYEN H.V.: 'Novel broadband dual-CRLH metamaterial: properties, implementation and applications', *Appl. Phys. A*, 2007, **87**, (2), pp. 309–316

[13] RENNINGS A., LIEBIG T., CALOZ C., WOFF I.: 'Double-Lorentz transmission line metamaterial and its application to tri-band devices'. IEEE MTT-S Int. Microwave Symp. Dig., June 2007, pp. 1427–1430

doi: 10.1049/iet-map:20070180